

# Adjusting the chlorhexidine content of calcium phosphate coatings by electrochemically assisted co-deposition from aqueous solutions

D. Scharnweber · M. Flössel · R. Born · H. Worch

Received: 15 June 2006 / Accepted: 18 September 2006  
© Springer Science + Business Media, LLC 2007

**Abstract** Currently, a number of strategies to create either biologically active or antimicrobial surfaces of biomaterials are being developed and commercially applied. However, for metallic implants in contact with bone, both osteomyelitis and a fast and stable long-term fixation of implants are challenges to be overcome, especially in the case of bad bone quality. Therefore, the present work aims to develop compound coatings of calcium phosphate phases (CPP) and chlorhexidine (CHD) that combine bioactive properties with a strategy to prevent initial bacterial adhesion and thus offer a possible solution to the two major problems of implant surgery mentioned above. Using electrochemically assisted deposition of CPP on samples of Ti6Al4V together with the pH-dependent solubility of CHD, the preparation of coatings with a wide range of CHD concentrations (150 ng/cm<sup>2</sup> to 65 μg/cm<sup>2</sup>) from electrolytes with CHD concentrations between 50 and 200 μM was possible, thus allowing the adaptation of implant surface properties to different surgical and patient situations. Detailed SEM and FTIR analysis showed that coatings are formed by a co-deposition process of both phases and that CHD interacts with the deposition and transformation of CPP in the coating. For high CHD contents, coatings consist of CHD crystals coated by nano-crystalline hydroxyapatite.

## Introduction

For implant surfaces in contact with bone, two property profiles are of special interest for clinical application. Firstly,

implant associated infections caused by staphylococci often result in acute and chronic osteomyelitis that can be difficult to treat and thus should be avoided by antimicrobial properties of implant surfaces. Secondly, for fast and adequate bone response to implant surfaces together with appropriate long-term behaviour, implant surfaces should be bioactive with respect to bone formation, e.g. due to surface coatings of calcium phosphate phases (CPP).

In the area of anti-infective treatments, thanks to its antibacterial properties (against a wide variety of gram-negative and gram-positive organisms, facultative anaerobes, aerobes, and yeast), chlorhexidine (CHD) (1,1'-Hexamethylenbis[5-(4-chlorophenyl)-biguanid]) is widely used in a number of dental applications to reduce inflammation as well as swelling of gums and gum bleeding [1–3]. In addition to such external applications, besides the use of antibiotics [4], a number of attempts have been made to apply CHD in the preparation of antibacterial implant surfaces [5–9].

While Dennison et al. [9] applied CHD in a simple way by treating implant surfaces with cotton pellets soaked with a 0.12% solution to test the effectivity of different cleaning treatments, Darauiche et al. [7] prepared antiseptic coatings of CHD on titanium cylinders together with chloroxylenol resulting in an inhibition effect against different staphylococci for up to 8 weeks after incubation. In a recent paper of Richards and his group [6], a number of different coatings systems providing up to 2 mg CHD per sample were tested with respect to the adhesion of fibroblasts and staphylococcal strains. With no intact fibroblasts observed on CHD impregnated surfaces, fewer bacteria were detected both in the surrounding media and on these surfaces compared to surfaces without CHD. Based on the release behaviour, PDLLA and PTF coatings are favoured for further investigations. DeJong et al. [8] directly combined HA and CHD by using a lipid-stabilized coating on external fixator pins in a

D. Scharnweber (✉) · M. Flössel · R. Born · H. Worch  
Max Bergmann Center of Biomaterials, Technische Universität,  
Dresden, Budapester Str. 27, 01069 Dresden, Germany  
e-mail: dieter.scharnweber@tu-dresden.de

goat model. While infection developed in 100% of uncoated pins, coated pins demonstrated an infection rate of only 4.2%, while 12.5% showed colonization and the remaining 83.3% no growth.

To provide osteoconductive properties to implant surfaces in contact with bone, besides current research in the field of matrix engineering using components of the extracellular matrix [10–17] and compounds derived thereof [18–23], coatings from CPP are well established. Of the different methods used for preparation of coatings from CPP [24–26] in recent years the electrochemically assisted deposition (ECAD) has grown in importance because of the advantageous properties of the resulting coatings and the favourable results from animal experiments [27–30] and clinical studies [31–33]. Thus, ECAD allows preparation of very thin coatings from brushite [34–39], amorphous calcium phosphate (ACP) [40, 41], octacalciumphosphate [42–46], and a number of different apatite stoichiometries [39–41, 43]. Using appropriate processing conditions, compound coatings with proteins [20, 47–49] and other organic components like chitosan [50–52] have also been prepared and characterized.

To combine bioactivity provided by CPP with the antimicrobial properties of CHD hence, the aim of this project was to develop a method for the preparation of coatings on metallic implants for contact with bone that (i) are based on a co-deposition of CHD with CPP allowing the integration of defined amounts of CHD into the coatings, (ii) are expected to improve healing behaviour of antimicrobial coatings by using CPP as biologically active compounds, and (iii) allow their release behaviour to be modified. To overcome these challenges we have developed a co-deposition process for CPP and CHD by electrochemically assisted deposition from aqueous solutions at body temperature.

## Materials and methods

The preparation of the samples as well as the deposition of the CPP layers was performed as previously described [40, 41]. All chemicals used were analytical grade.

In brief, the surfaces of samples from Ti6Al4V (diameter 10 mm, height 2 mm) were prepared by grinding and polishing, using a titanium oxide suspension (anatase, particle size 20 nm) as the final step. Before use, ultrasonic cleaning was performed using 1% Triton X-100, acetone and ethanol for 15 min each.

A combined potentiostat/galvanostat unit (model 273A, EG&G, USA) coupled with a double-walled electrochemical cell that ensured constant temperature during polarisation was used in the experiments. A platinum net served as counter electrode. Cathodic polarisation was performed in the galvanostatic mode with current densities of 5 and 7.5 mA/cm<sup>2</sup> used for 10 and 60 minutes respectively at 36°C. The elec-

trolyte used for CPP deposition was prepared from 0.0333 M CaCl<sub>2</sub> and 0.02 M NH<sub>4</sub>H<sub>2</sub>PO<sub>4</sub> (Fluka, Neu-Ulm, Germany) by diluting equal volumes at a ratio of 1: 20 in distilled water. The final pH of the electrolyte was adjusted to 6.4 with ammonium hydroxide solution (Merck, Darmstadt, Germany). Chlorhexidine (molecular weight 505.5 g/Mol, Sigma-Aldrich, Germany) was added to the electrolyte for the CPP deposition with concentrations of 50, 100, and 200 μM respectively. Coatings were rinsed with distilled water and allowed to dry in air.

Deposited coatings have been investigated using scanning electron microscopy (SEM) (DSM 982 Gemini, Carl Zeiss, Oberkochen, Germany) with 1 keV acceleration voltage and FT-IR spectroscopy (Perkin Elmer FTS 2000 equipped with an Autoimage Microscope, Boston, USA). The CHD content of the coatings was determined by UV-VIS spectrometry (Spectrometer Lambda 10, Perkin Elmer, Boston, USA) at 270 nm after dissolution of the coatings in 0.01 M nitric acid using quartz cuvettes of 1 cm optical path length.

## Results

### CHD content

Co-deposition of CHD and CPP has been performed from electrolytes with variable concentrations of CHD using two current densities and deposition times. The amount of CHD as detected from the dissolution of CHD containing CPP layers in this parameter field is given in Fig. 1. For short deposition times (10 min) the deposited amount of CHD (between 0.15 and 0.5 μg/cm<sup>2</sup>) is nearly independent of the CHD concentration in the electrolyte, with the applied current density having only a weak effect on the deposited amount of CHD.

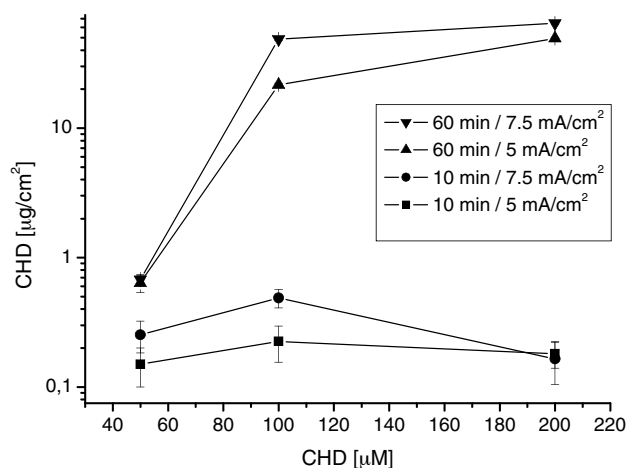


**Fig. 1** Amount of CHD deposited during cathodic polarisation as function of the CHD concentration of the electrolyte, the current density applied, and the deposition time

Whereas for 200  $\mu\text{M}$  no differences in the CHD masses are detected, the current density of 7.5  $\text{mA}/\text{cm}^2$  results in approximately twofold higher CHD masses in the layers compared to 5  $\text{mA}/\text{cm}^2$  for electrolyte concentrations of 50 and 100  $\mu\text{M}$  CHD.

For a deposition time of 60 min a (weak) influence of the current density on the deposited amount of CHD is only detected for electrolyte 100  $\mu\text{M}$  in CHD. However for this deposition time the deposited amount of CHD is strongly influenced by the CHD concentration of the electrolyte with an increase in the CHD concentration of the electrolyte by a factor of two (50 to 100  $\mu\text{M}$ ) resulting in at least 20-fold higher CHD masses in the coatings (from about 0.8  $\mu\text{g}/\text{cm}^2$  to 20–50  $\mu\text{g}/\text{cm}^2$ ). Doubling the CHD concentration of the electrolyte again (100 to 200  $\mu\text{M}$ ) yields only a slight further increase of the deposited mass of CHD. In general, depending on the current density during the electrochemically assisted deposition, the polarisation time, and the CHD concentration in the electrolyte, the CHD content of the coatings varied over nearly three orders of magnitude between 150  $\text{ng}/\text{cm}^2$  and 65  $\mu\text{g}/\text{cm}^2$ .

Whereas CHD amounts in the  $\text{ng}/\text{cm}^2$  range could not be detected in the layers by microscopic techniques, coatings containing CHD in the  $\mu\text{g}/\text{cm}^2$  range show needles with a length of up to 100  $\mu\text{m}$  and a diameter of about 300 nm that are almost completely coated by nano-crystalline hydroxyapatite (HA) (Figs. 2 and 3). On more detailed examination of Fig. 2, the different CHD masses of 22 and 50  $\mu\text{g}/\text{cm}^2$  for the coatings deposited with a current density of 5  $\text{mA}/\text{cm}^2$  for 60 min from electrolytes containing 100 and 200  $\mu\text{M}$  CHD respectively (see Fig. 1) are clearly reflected by the appearance of the coatings. Whereas for the coating with 22  $\mu\text{g}/\text{cm}^2$  CHD (Fig. 2 (a)) only a few agglomerates from CHD needles are present, the sample with 50  $\mu\text{g}/\text{cm}^2$  is fully covered with agglomerated CHD needles forming a partially interlocking network.

#### CPP phase composition of layers

The type of the deposited CPP as a function of the parameters CHD concentration, current density, and deposition time has been followed by SEM and FT-IR spectroscopy. Independently of the electrolyte composition and the current conditions, amorphous calcium phosphate (ACP) as identified by FT-IR and in comparison to former experiments [40] is present for a deposition time of 10 min. However the size of the globular ACP spheres increases in the presence of CHD and with increasing CHD concentration. Thus, spheres prepared in the presence of 200  $\mu\text{M}$  CHD are on average larger in diameter by a factor of about 4 compared to those precipitated from electrolytes without CHD as shown in Fig. 4. Interestingly, the large spheres grown in the presence

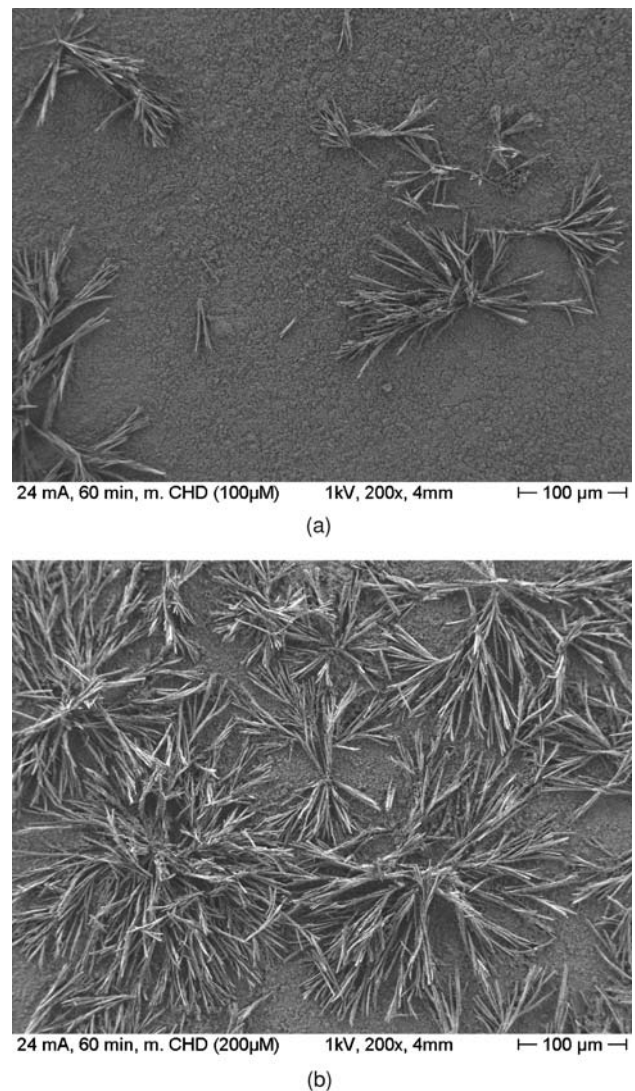


**Fig. 2** SEM images of CPP/CHD coatings deposited with 5  $\text{mA}/\text{cm}^2$  for 60 min: (a) from 100  $\mu\text{M}$  CHD electrolyte; (b) from 200  $\mu\text{M}$  CHD electrolyte

of CHD are clearly structured and seem to be composed of sub-spheres.

Figure 5 reflects a second effect of the presence of CHD on the precipitation of CPP. Whereas for the electrolyte without CHD, for a polarisation time of 60 min, the coating already consists nearly completely of HA, in the presence of 50  $\mu\text{M}$  CHD in the coating, still, mainly ACP is present. This behaviour is observed only for the lowest CHD concentration and the current density of 5  $\text{mA}/\text{cm}^2$ , for higher CHD concentrations and/or for the current density of 7.5  $\text{mA}/\text{cm}^2$  the coatings consist mostly of HA, showing only a few ACP spheres for the parameter sets [50  $\mu\text{M}$  & 7.5  $\text{mA}/\text{cm}^2$ ] and [100  $\mu\text{M}$  & 5  $\text{mA}/\text{cm}^2$ ].

Figure 6 gives FT-IR spectra for coatings prepared for 10 and 60 min respectively with a current density of 5  $\text{mA}/\text{cm}^2$  in an electrolyte 200  $\mu\text{M}$  in CHD, thus corresponding to Figs.

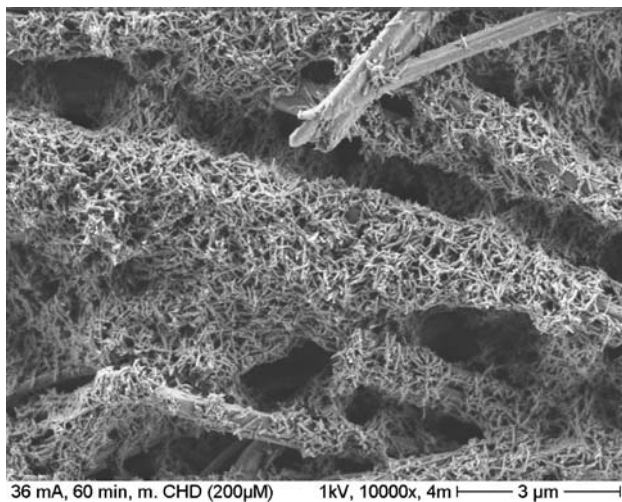


**Fig. 3** Detailed SEM image of CHD crystals embedded in a hydroxyapatite coating; deposition parameters  $7.5 \text{ mA/cm}^2$  for 60 min from  $200 \mu\text{M}$  CHD electrolyte

4(a) and 2(b). Whereas the phosphate peak around  $1050 \text{ cm}^{-1}$  shows no sub-structure for the short deposition time because of the ACP coating, it is clearly split into a maximum at  $1030 \text{ cm}^{-1}$  and a shoulder at  $1110 \text{ cm}^{-1}$  for the deposition time of 60 min indicating the presence of hydroxyapatite. The spectrum for the longer deposition time additionally contains a number of maxima around 800, at  $1250$ , and between  $1350$  and  $1600 \text{ cm}^{-1}$ , which can be assigned to CHD and reflect the higher CHD content of this coating. For the short deposition time CHD can hardly be detected in the FT-IR spectrum.

## Discussion

Coatings on implant surfaces for contact with bone have to fulfil several tasks. Besides preventing bacterial adhesion they should have an osteoconductive or even -inductive potential. To combine these properties in one coating, a co-deposition method for the preparation of CHD/ACP compound coatings with a wide variation in the CHD content has been developed. The basic principle of the method is the electrochemical assisted deposition of ACP, i.e. a cathodic polarization of the substrate in aqueous solutions containing Ca and phosphate ions. This polarization raises the pH on the surface and thus induces the deposition of ACP due to their pH-dependent solubility.

By changing the electrochemical parameters and the deposition time of the coatings from electrolytes whose CHD concentrations differed by a factor of four ( $50$  to  $200 \mu\text{M}$ ), coatings varying in the amount of CHD by a factor of over 400 ( $150 \text{ ng/cm}^2$  to  $65 \mu\text{g/cm}^2$ ) could be deposited. For coatings with CHD contents in the  $\mu\text{g}$  range, needle-like CHD crystals with a length of up to  $100 \mu\text{m}$  and a diameter of about

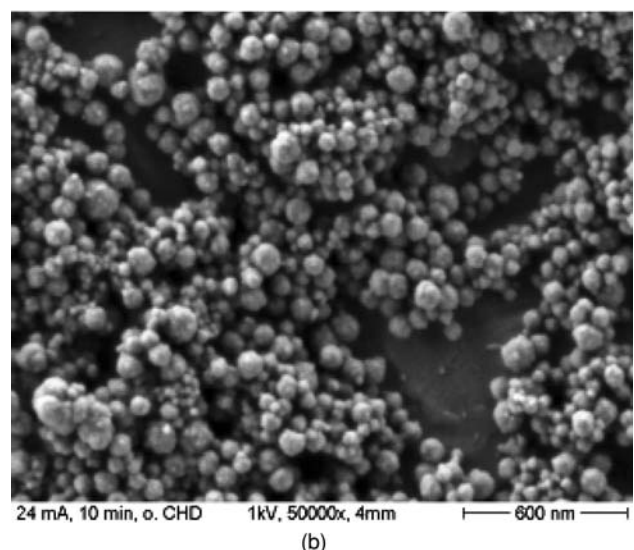
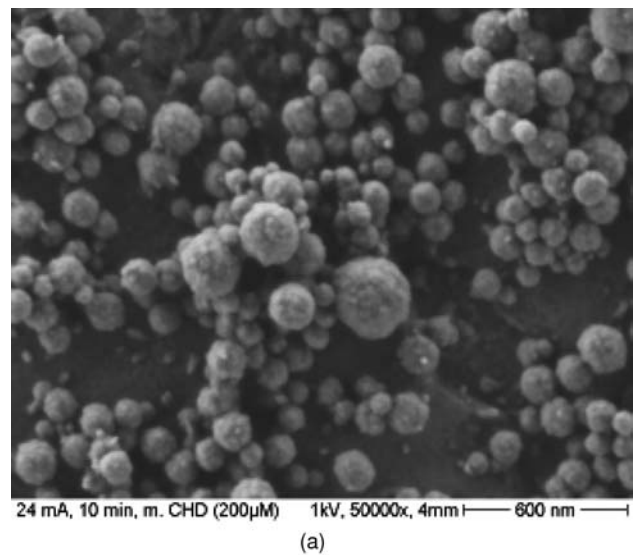
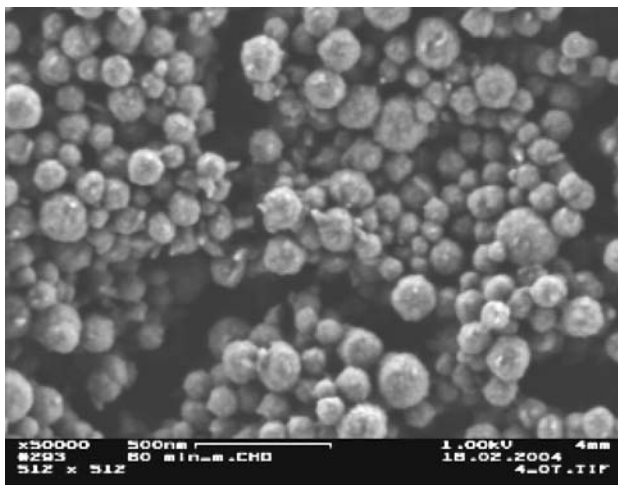


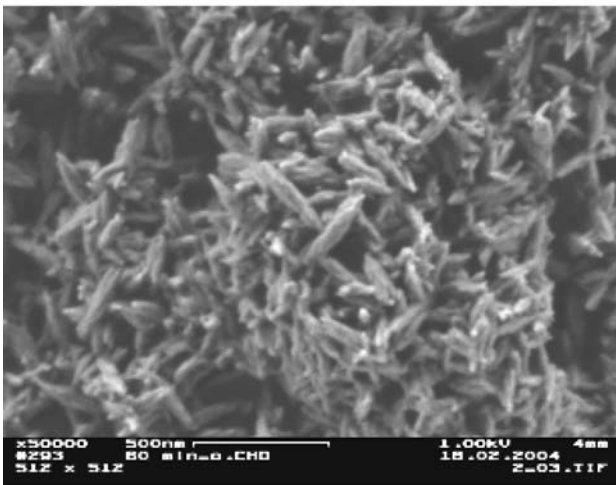
**Fig. 4** Coatings from ACP prepared with  $i = 5 \text{ mA/cm}^2$  and  $t = 10 \text{ min}$ : (a) with  $200 \mu\text{M}$  CHD; (b) without CHD

$300 \text{ nm}$ , which are almost completely coated by nanocrystalline hydroxyapatite, are present in the compound layers. The morphology of this HA is not significantly changed when compared to that deposited from similar electrolytes without CHD [40, 41, 53, 54].

Both the increase of the CHD content of the coatings, which is disproportionately large in comparison to the increase in electrolyte concentrations of CHD ( $>400$  to  $4$ ), and the presence of CHD crystals on the surfaces for sufficient polarization time indicate that the incorporation of CHD into the coatings is positively influenced by cathodic polarization. The most probable explanation is a pH-dependent solubility of CHD as suggested by Jones et al. [55]. These authors investigated the state of CHD in different semisolids by Raman spectroscopy. From peak shifts of the strongest



(a)



(b)

**Fig. 5** CPP coatings prepared with  $i = 5 \text{ mA/cm}^2$  and  $t = 60 \text{ min}$ : (a) with  $50 \mu\text{M}$  CHD; (b) without CHD

band from  $1564$  to  $1608 \text{ cm}^{-1}$  they suggest an enhanced solubility of the protonated cation  $\text{H}_2\text{CHD}^{2+}$ , corresponding to a decreasing solubility of CHD with increasing pH. Thus the formation of compound coatings from CHD and HA can be described as similar to that of coatings of CPP and chitosan [50–52]. Chitosan is also present as a cation in slightly acidic solutions.

As shown in Fig. 1, high CHD contents of the coatings, combined with crystals from CHD, are present only for the long polarization time and CHD concentrations above  $50 \mu\text{M}$ . Thus, both sufficient polarization time and CHD concentration in the electrolyte are prerequisites for the formation of such crystals.

Interestingly, the presence of crystals from CHD is always associated with coatings from nano-crystalline HA and from the experiments with a current density of  $5 \text{ mA/cm}^2$  for 60 min in electrolytes with/without  $50 \mu\text{M}$  CHD it has to be

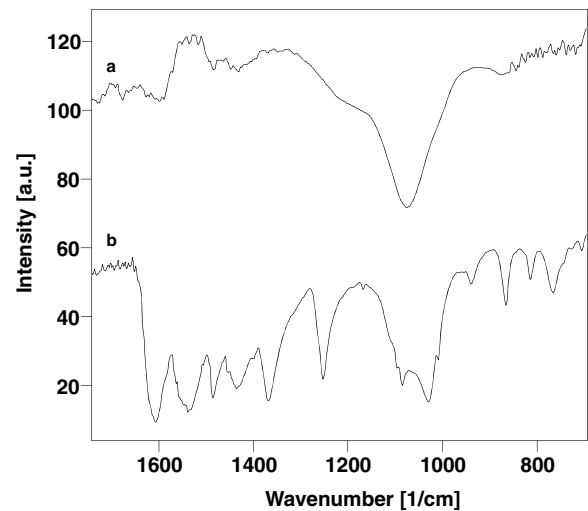


**Fig. 6** FT-IR spectra of coatings prepared with a current density of  $5 \text{ mA/cm}^2$  in electrolyte with a CHD concentration of  $200 \mu\text{M}$ : (a) spectrum for a ACP coating with 10 min deposition time; (b) spectrum for a HA coating with 60 min deposition time

concluded that the transformation of ACP into HA is hampered under these conditions (see Fig. 5). Correspondingly it was found that the size of the ACP spheres is increased in the presence of CHD (see Fig. 3). Thus it can be speculated that the co-deposition of CHD with ACP in the initial phase of the formation of the coatings results in strong interactions between both components and thus interferes with both the transformation of ACP into HA as described in [40] in great detail and the formation of crystals from CHD. With that in mind, the transformation of ACP into HA seems to be a prerequisite for the crystallization of CHD and thus the realization of higher CHD contents in the coatings. How this transformation can be influenced by a number of additional factors such as electrolyte composition, deposition time, and current density have been studied in [40, 41] for the conditions used in this work. Besides, the process temperature also plays a major role in the deposition of crystalline CPP as shown in [56]. Thus choosing right combinations of these parameters should allow tailoring the CPP/CHD ratios in the layers according to the specific needs of patients.

## Conclusions

CHD as a cationic antibacterial agent for the first time has been co-deposited with CPP in an electrochemically assisted process due to its pH-dependent solubility, which allows variation of the CHD content of the coatings over several orders of magnitude. While coatings with low concentrations of CHD can be prepared by co-deposition of CHD with ACP, higher contents of CHD can be realized by co-crystallization of CHD and HA. Further influencing the release behaviour of

CHD-layered coatings by combining deposition from electrolytes with/without CHD could be envisaged. Work in relation to this, together with the characterisation of the release behaviour of CHD from the coatings, is currently in progress. This will have to be followed by cytotoxicity investigations as already performed by a number of authors [6, 57, 58].

## References

1. G. CARLO CESCHEL, V. BERGAMANTE, V. CALABRESE, S. BISERNI, C. RONCHI and A. FINI, *Drug. Dev. Ind. Pharm.* **32** (2006) 53.
2. L. B. FREITAS, J. RUNDEGREN and T. ARNEBRANT, *Oral Microbiol. Immunol.* **8** (1993) 355.
3. D. N. MISRA, *J. Biomed. Mater. Res.* **28** (1994) 1375.
4. M. DIEFENBECK, T. MUCKLEY and G. O. HOFMANN, *Injury* **37** (2006) S95.
5. M. MORRA, C. CASSINELLI, G. CASCARDO, A. CARPI, M. FINI, G. GIAVARESI and R. GIARDINO, *Biomed. Pharmacot.* **58** (2004) 418.
6. L. G. HARRIS, L. MEAD, E. MULLER-OBERLANDER and R. G. RICHARDS, *J. Biomed. Mater. Res.* **78A** (2006) 50.
7. R. O. DAROUICHE, G. GREEN and M. D. MANSOURI, *Int. J. Antimicrob. Agents* **10** (1998) 83.
8. E. S. DEJONG, T. M. DEBERARDINO, D. E. BROOKS, B. J. NELSON, A. A. CAMPBELL, C. R. BOTTONI, A. E. PUSATERI, R. S. WALTON, C. H. GUYMON and A. T. MCMANUS, *J. Trauma* **50** (2001) 1008.
9. D. K. DENNISON, M. B. HUERZELER, C. QUINONES and R. G. CAFFESSE, *J. Periodontol.* **65** (1994) 942.
10. S. BIERBAUM, R. BEUTNER, T. HANKE, D. SCHARNWEBER, U. HEMPEL and H. WORCH, *J. Biomed. Mater. Res.* **67A** (2003) 421.
11. S. BIERBAUM, T. DOUGLAS, T. HANKE, D. SCHARNWEBER, S. TIPPELT, T. K. MONSEES, R. H. FUNK and H. WORCH, *J. Biomed. Mater. Res.* **77A** (2006) 551.
12. S. BIERBAUM, U. HEMPEL, U. GEISLER, T. HANKE, D. SCHARNWEBER, K. WENZEL and H. WORCH, *J. Biomed. Mater. Res.* **67A** (2003) 431.
13. U. GEISLER, U. HEMPEL, C. WOLF, D. SCHARNWEBER, H. WORCH and K. WENZEL, *J. Biomed. Mater. Res.* **51** (2000) 752.
14. M. WOLLENWEBER, H. DOMASCHKE, T. HANKE, S. BOXBERGER, G. SCHMACK, K. GLIESCHE, D. SCHARNWEBER and H. WORCH, *Tissue Eng.* **12** (2006) 345.
15. R. MÜLLER, J. ABKE, E. SCHNELL, D. SCHARNWEBER, R. KUJAT, C. ENGLERT, D. TAHERI, M. NERLICH and P. ANGELE, *Biomaterials* **27** (2006) 4059.
16. M. MORRA, C. CASSINELLI, L. MEDA, M. FINI, G. GIAVARESI and R. GIARDINO, *Int. J. Oral Maxillofac. Implants* **20** (2005) 23.
17. M. NAGAI, T. HAYAKAWA, A. FUKATSU, M. YAMAMOTO, M. FUKUMOTO, F. NAGAHAMA, H. MISHIMA, M. YOSHINARI, K. NEMOTO and T. KATO, *Dent. Mater. J.* **21** (2002) 250.
18. J. AUERNHEIMER, D. ZUKOWSKI, C. DAHMEN, M. KANTLEHNER, A. ENDERLE, S. L. GOODMAN and H. KESSLER, *ChemBiochem* **6** (2005) 2034.
19. C. DAHMEN, J. AUERNHEIMER, A. MEYER, A. ENDERLE, S. L. GOODMAN and H. KESSLER, *Angew. Chem. Int. Ed.* **43** (2004) 6649.
20. S. RÖSSLER, R. BORN, D. SCHARNWEBER, H. WORCH, A. SEWING and M. DARD, *J. Mater. Sci.: Mater. Med.* **12** (2001) 871.
21. H. SCHLIEPHAKE, D. SCHARNWEBER, M. DARD, S. RÖSSLER, A. SEWING, J. MEYER and D. HOOGESTRAAT, *Clin. Oral. Implants. Res.* **13** (2002) 312.
22. M. SCHULER, G. R. OWEN, D. W. HAMILTON, M. DE WILD, M. TEXTOR, D. M. BRUNETTE and S. G. TOSATTI, *Biomaterials* **27** (2006) 4003.
23. U. MAGDOLEN, J. AUERNHEIMER, C. DAHMEN, J. SCHAUWECKER, H. GOLLWITZER, J. TUBEL, R. GRADINGER, H. KESSLER, M. SCHMITT and P. DIEHL, *Int. J. Mol. Med.* **17** (2006) 1017.
24. L. SUN, C. C. BERNDT, K. A. GROSS and A. KUCUK, *J. Biomed. Mater. Res.* **58** (2001) 570.
25. R. J. TALIB and M. R. TOFF, *Med. J. Malaysia* **59**(Suppl. B) (2004) 153.
26. T. KOKUBO, H. M. KIM, M. KAWASHITA and T. NAKAMURA, *J. Mater. Sci.: Mater. Med.* **15** (2004) 99.
27. S. BAN, S. MARUNO, N. ARIMOTO, A. HARADA and J. HASEGAWA, *J. Biomed. Mater. Res.* **36** (1997) 9.
28. J. REDEPENNING, T. SCHLESSINGER, S. BURNHAM, L. LIPPIELLO and J. MIYANO, *J. Biomed. Mater. Res.* **30** (1996) 287.
29. H. SCHLIEPHAKE, D. SCHARNWEBER, M. DARD, S. RÖSSLER, A. SEWING and C. HUTTMANN, *J. Biomed. Mater. Res.* **64A** (2003) 225.
30. S. SZMUKLER-MONCLER, D. PERRIN, V. AHOSSI and P. POINTAIRE, *Key Eng. Mater.* **192**(1) (2001) 395.
31. B. BIRKENHAUER, H. KISTMACHER and J. RIES, *Orthopäde* **33** (2004) 1259.
32. J. MOCKWITZ and V. DATHE, *Orthopädische Praxis* **38** (2002) 260.
33. P. L. WOOD and S. DEAKIN, *J. Bone Joint Surg.* **85** (2003) 334.
34. H. NEUMANN, U. BECK, M. DRAWER and J. STEINBACH, *Surf. Coat. Technol.* **98** (1998) 1157.
35. J. REDEPENNING and J. MCISAAC, *Chem. Mater.* **2** (1990) 625.
36. L. HUANG, K. XU and J. LU, *J. Mater. Sci.: Mater. Med.* **11** (2000) 667.
37. Y. HAN, K. XU and J. LU, *J. Mater. Sci.: Mater. Med.* **10** (1999) 243.
38. H. BENHAYOUNE, P. LAQUERRIERE, E. JALLOT, A. PERCHET, L. KILIAN, G. BALOSSIER, J. L. BUBENDORFF and G. D. SOCKALINGUM, *J. Mater. Sci. Mater. Med.* **13** (2002) 1057.
39. M. SHIRKHAZADEH, *J. Mater. Sci.: Mater. Med.* **6** (1995) 90.
40. S. RÖSSLER, A. SEWING, M. STÖLZEL, R. BORN, D. SCHARNWEBER, M. DARD and H. WORCH, *J. Biomed. Mater. Res.* **64A** (2003) 655.
41. A. SEWING, M. LAKATOS, D. SCHARNWEBER, S. RÖSSLER, R. BORN, M. DARD and H. WORCH, *Bioceramics* **16** (2004) 419.
42. S. BAN, S. MARUNO, A. HARADA, M. HATTORI, K. NARITA and J. HASEGAWA, *Dent. Mater. J.* **15** (1996) 31.
43. J. LEGEROS, S. LIN, D. MIJARES, F. DIMAANO and R. LEGEROS, *Bioceramics* **17** (2005) 247.
44. S. LIN, R. Z. LEGEROS and J. P. LEGEROS, *J. Biomed. Mater. Res.* **66A** (2003) 819.
45. Q. ZHANG and Y. LENG, *Biomaterials* **26** (2005) 3853.

46. Q. ZHANG, Y. LENG and R. XIN, *Biomaterials* **26** (2005) 2857.
47. X. CHENG, M. FILIAGGI and S. G. ROSCOE, *Biomaterials* **25** (2004) 5395.
48. Y. FAN, K. DUAN and R. WANG, *Biomaterials* **26** (2005) 1623.
49. H. OKAMURA, M. YASUDA and M. OHTA, *Electrochemistry* **68** (2000) 486.
50. J. REDEPENNING, G. VENKATARAMAN, J. CHEN and N. STAFFORD, *J. Biomed. Mater. Res.* **66A** (2003) 411.
51. J. WANG, J. DE BOER and K. DE GROOT, *J. Dent. Res.* **83** (2004) 296.
52. J. WANG, A. VAN APELDOORN and K. DE GROOT, *J. Biomed. Mater. Res.* **76A** (2006) 503.
53. R. BORN, D. SCHARNWEBER, S. RÖSSLER, M. STÖLZEL, M. THIEME, C. WOLF and H. WORCH, *Fres. J. Anal. Chem.* **361** (1998) 697.
54. H. WORCH and D. SCHARNWEBER, *Z. Metallkunde* **89** (1998) 153.
55. D. S. JONES, A. F. BROWN, A. D. WOOLFSON, A. C. DENNIS, L. J. MATCHETT and S. E. BELL, *J. Pharm. Sci.* **89** (2000) 563.
56. S. BAN and S. MARUNO, *Biomaterials* **16** (1995) 977.
57. P. GOLDSCHMIDT, R. COGEN and S. TAUBMAN, *J. Periodontol* **48** (1977) 212.
58. I. R. SANCHEZ, K. E. NUSBAUM, S. F. SWAIM, A. S. HALE, R. A. HENDERSON and J. A. MCGUIRE, *Vet. Surg.* **17** (1988) 182.